***Graphical Abstract - Pictogram**

$$\mathrm{ReO_4^- + 2\ SF_4 \xrightarrow{CH_3CN} ReO_2F_4^- + 2\ SOF_2}$$

$$\mathrm{IO_3^- + 2\ SF_4 \xrightarrow{CH_3CN} IOF_4^- + 2\ SOF_2}$$

$$\mathrm{IO_4^- + 2\ SF_4 \xrightarrow{aHF} IO_2F_4^- + 2\ SOF_2}$$

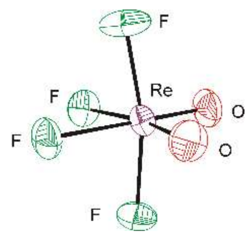

***Graphical Abstract - Synopsis**

The reaction of $AgReO_4$, $[N(CH_3)_4]IO_3$, and KIO_4 with SF_4 in an appropriate solvent yields pure $Ag[ReO_2F_4]$, $[N(CH_3)_4][IOF_4]$, and $K[IO_2F_4]$, respectively, in a single step.

Suflur tetrafluoride is of great utility for inorganic chemistry.

Rhenium and iodine oxide fluoride salts can be prepared using SF_4 as a reagent.

$Ag[Re_2O_2F_4]$ forms coordination compounds with CH_3CN.

A New Synthetic Route to Rhenium and Iodine Oxide Fluoride Anions: The Reaction between Oxoanions and Sulfur Tetrafluoride

James T. Goettel,[a,b] Douglas Turnbull,[a,b] and Michael Gerken[a,b,*]

[a] *Department of Chemistry and Biochemistry, The University of Lethbridge, Lethbridge, Alberta, T1K 3M4, Canada*

[b] *Canadian Centre for Research in Advanced Fluorine Technologies, The University of Lethbridge, Lethbridge, Alberta, T1K 3M4, Canada*

* Corresponding author. Tel.: +1-403-329-2173; fax: +1-403-329-2057. *e-mail address*: michael.gerken@uleth.ca.

Abstract

Sulfur tetrafluoride is a reagent for the one-step syntheses of $[Re^{VII}O_2F_4]^-$, $[I^{V}OF_4]^-$, and $[I^{VII}O_2F_4]^-$ salts. Pure $Ag[ReO_2F_4]$ as well as its CH_3CN coordination compounds were obtained from CH_3CN solvent. The $Ag[ReO_2F_4]$, $[Ag(CH_3CN)_2][ReO_2F_4]$ and $[Ag(CH_3CN)_4][ReO_2F_4]$ salts were characterized by Raman spectroscopy. The $[Ag(CH_3CN)_4][ReO_2F_4]\cdot 2CH_3CN$ coordination compound was characterized by single-crystal X-ray diffraction. The reaction of SF_4 with KIO_4 in anhydrous HF gave the known $K[IO_2F_4]$ salt. The reaction of $[N(CH_3)_4]IO_3$ with SF_4 in CH_3CN yielded the new $[N(CH_3)_4][IOF_4]$ salt, which was characterized by Raman spectroscopy.

1. Introduction

Sulfur tetrafluoride has extensively been used as a fluorinating agent in organic chemistry.[1] The utility of SF_4 in inorganic chemistry had been explored for converting metal oxides to fluorides at high temperatures and pressures.[2] For example, Bi_2O_3, TiO_2, U_3O_8, and HgO are fluorinated by SF_4 to BiF_3 (Eq. 1), TiF_4, UF_6, and HgF_2, respectively.

$$Bi_2O_3 + 3\ SF_4 \quad \rightarrow \quad 2\ BiF_3 + 3\ SOF_2 \qquad (1)$$

Main-group and transition-metal sulfides also react with SF_4 to produce fluorides (SnS_2 to SnF_4 and FeS_2 to FeF_2) and some oxides were shown to be converted to oxide fluorides (P_4O_{10} to POF_3) (see Eqs 2 and 3, respectively).

$$SnS_2 + SF_4 \quad \rightarrow \quad SnF_4 + 3/8\ S_8 \qquad (2)$$

$$P_4O_{10} + 6\ SF_4 \quad \rightarrow \quad 4\ POF_3 + 6\ SOF_2 \qquad (3)$$

Sulfur tetrafluoride will generally react in a metathesis reaction transferring two of its fluorines when reacting with oxides. In reactions of SF_4 with sulfides, comproportionation reactions are observed where all four fluorines are transferred. Very little has been reported on the use of SF_4 as a fluorinating agent towards oxoanions of main-group and transition-metal elements in high oxidation states.[3]

A large number of oxide fluoride anions have been synthesized and characterized.[4] The $ReO_2F_4^-$ anion, with rhenium in its highest oxidation state, was first synthesized in 1955 by Peacock from the reaction of excess BrF_3 with metal perrhenate salts (see Eq 4).[5]

$$3\ ReO_4^- + 4\ BrF_3 \quad \rightarrow \quad 3\ ReO_2F_4^- + 3\ O_2 + 2\ Br_2 \qquad (4)$$

The reaction required extensive heating under vacuum to remove excess unreacted BrF_3 and the Br_2 byproduct. Another method of synthesizing the $ReO_2F_4^-$ anion is through the reaction of ReO_2F_3 with fluoride salts, such as MF (M = Li, Na, K, Cs) and $[N(CH_3)_4]F$.[6] The $ReO_2F_4^-$ salts were characterized by Raman spectroscopy, while $Li[ReO_2F_4]$ was also characterized by single crystal X-ray diffraction.[6] Neutral ReO_2F_3 can be prepared by the reaction of Re_2O_7 with XeF_6 in anhydrous HF. Holloway *et al.* report that $KReO_4$ does not react with anhydrous HF at room temperature,[7] whereas Seppelt *et al.* report the reaction yields $ReO_2F_4^-$.[8] Another paper mentions the formation of ReO_3F in the reaction of $KReO_4$ with anhydrous HF.[9] As a matter of fact, these different rhenium(VII) species are in equilibrium with each other in aHF, therefore, a large excess of aHF is required to produce $ReO_2F_4^-$ and the yields are low.

Iodine can form a number of oxide fluoride anions in the +5 and +7 oxidation states. Previous syntheses of the IOF_4^- anion include the reaction of IF_5 with a metal fluoride and iodate, or hydrolysis of the IF_6^- anion.[10] These reactions, however, produced mixtures of $IO_2F_2^-$ and IOF_4^- anions. Christe *et al.* have prepared pure Li^+, Na^+, K^+, Rb^+, and NO^+ salts of the IOF_4^- anion by reaction of I_2O_5 with IF_5 in the presence of the respective fluoride salt,[11,12] while $Li[IOF_4]$, $K[IOF_4]$ and $Cs[IOF_4]$ were also prepared from IF_5 and the respective NO_3^- salts, however, in admixture with reaction byproducts.[12] The alkali metal salts of IOF_4^- were characterized by vibrational spectroscopy.[12] Only the crystal structure of $Cs[IOF_4]$ has been reported, which was the product of accidental hydrolysis.[13] The $IO_2F_4^-$ anion was previously synthesized by the repeated treatment of IO_4^- with aHF followed by removal of all volatiles.[14] An alternative route is the reaction of IO_2F_3 with $[N(CH_3)_4]F$ in acetonitrile, but this route is hazardous since detonations have occurred during this reaction.[15] Both of these methods of preparing the $IO_2F_4^-$ anion produced mixtures of *trans* and *cis* isomers.

2. Results and Discussion

The reactions of sulfur tetrafluoride with oxoanions of Re^{VII}, I^{V}, and I^{VII} were studied using Raman and NMR spectroscopy, as well as X-ray crystallography. No reaction between $AgReO_4$, $KReO_4$, KIO_4 or $[N(CH_3)_4]IO_3$ with neat SF_4 was observed at room temperature. The reaction between $AgReO_4$ and SF_4, however, proceeds at temperatures between −40 and 20 °C when CH_3CN is used as a solvent (see Eq 5).

$$AgReO_4 + 2\ SF_4 \quad \rightarrow \quad Ag[ReO_2F_4] + 2\ SOF_2 \qquad (5)$$

The reaction also proceeds for $KReO_4$ in CH_3CN solvent, but due to the poor solubility of $KReO_4$ in CH_3CN, the reaction is difficult to bring to completion. At −40 °C, a silver salt of $ReO_2F_4^-$ containing acetonitrile crystallizes from CH_3CN. The crystal structure of this salt showed four CH_3CN ligands coordinated to Ag^+ and two "free" solvent molecules per formula unit, resulting in a composition of $[Ag(CH_3CN)_4][ReO_2F_4]\cdot 2CH_3CN$ (*vide infra*). The uncoordinated CH_3CN can be easily removed under dynamic vacuum, yielding $[Ag(CH_3CN)_4][ReO_2F_4]$ as identified by Raman spectroscopy. The isolation of bulk amounts of $[Ag(CH_3CN)_4][ReO_2F_4]\cdot 2CH_3CN$ proved to be difficult. Removal of volatiles under dynamic vacuum at room temperature yields $[Ag(CH_3CN)_2][ReO_2F_4]$. The linear coordination of Ag^+ is a common coordination mode and the composition of the bis(acetonitrile)silver(I) salt is supported by the mass balance. Acetonitrile can be fully removed at 70 °C under dynamic vacuum, as shown by Raman spectroscopy. The $Ag[ReO_2F_4]$ salt obtained in the present study was a light cream-coloured solid. This is in contrast to Peacock's report that $Ag[ReO_2F_4]$ is a darker coloured salt than the other metal salts of $ReO_2F_4^-$, which may have been due to contamination.[5] No indication of photosensitivity of the $Ag[ReO_2F_4]$ salt was observed, when leaving $Ag[ReO_2F_4]$ exposed to sunlight for 3 days. The $Ag[ReO_2F_4]$ salt had previously only been characterized by its physical properties and elemental analysis.

The reaction between $[N(CH_3)_4]IO_3$ and SF_4 in acetonitrile at room temperature quantitatively yields the new IOF_4^- salt, $[N(CH_3)_4][IOF_4]$ (see Eq 6).

$$[N(CH_3)_4][IO_3] + 2\ SF_4 \rightarrow [N(CH_3)_4][IOF_4] + 2\ SOF_2 \qquad (6)$$

No reaction occurred between KIO_4 and SF_4 in acetonitrile. A slurry of KIO_4 in anhydrous HF reacted with SF_4 to form a clear colourless solution at 0 °C. When the volatiles were removed at −78 °C, colourless solid $K[IO_2F_4]$ was obtained. In anhydrous HF, an equilibrium between KIO_4 and $K[IO_2F_4]$ (Eq. 7) is operative, as previously utilized to prepare $IO_2F_4^-$ salts in several steps. Sulfur tetrafluoride likely acts to remove water (Eq. 8) from this reaction mixture shifting the equilibrium to the product side. In addition, SF_4 may react with the IO_4^- anion in a metathesis reaction.

$$KIO_4 + 2HF \rightleftarrows K[IO_2F_4] + H_2O \qquad (7)$$

$$H_2O + SF_4 \rightarrow 2HF + SOF_2 \qquad (8)$$

2.1. Raman Spectroscopy

The Raman spectra of $[Ag(CH_3CN)_x][ReO_2F_4]$ (where x = 0, 2, 4) are depicted in Figure 1. The Raman frequencies and tentative assignments are listed in Table 1. The signals associated with the acetonitrile moieties were assigned based on previous assignments made by Reedijk *et al.* [16] The signals associated with the $ReO_2F_4^-$ anion were assigned based on the previous assignments made by Schrobilgen *et al.*,[6] who used DFT calculations to aid in the assignment of the vibrational modes.

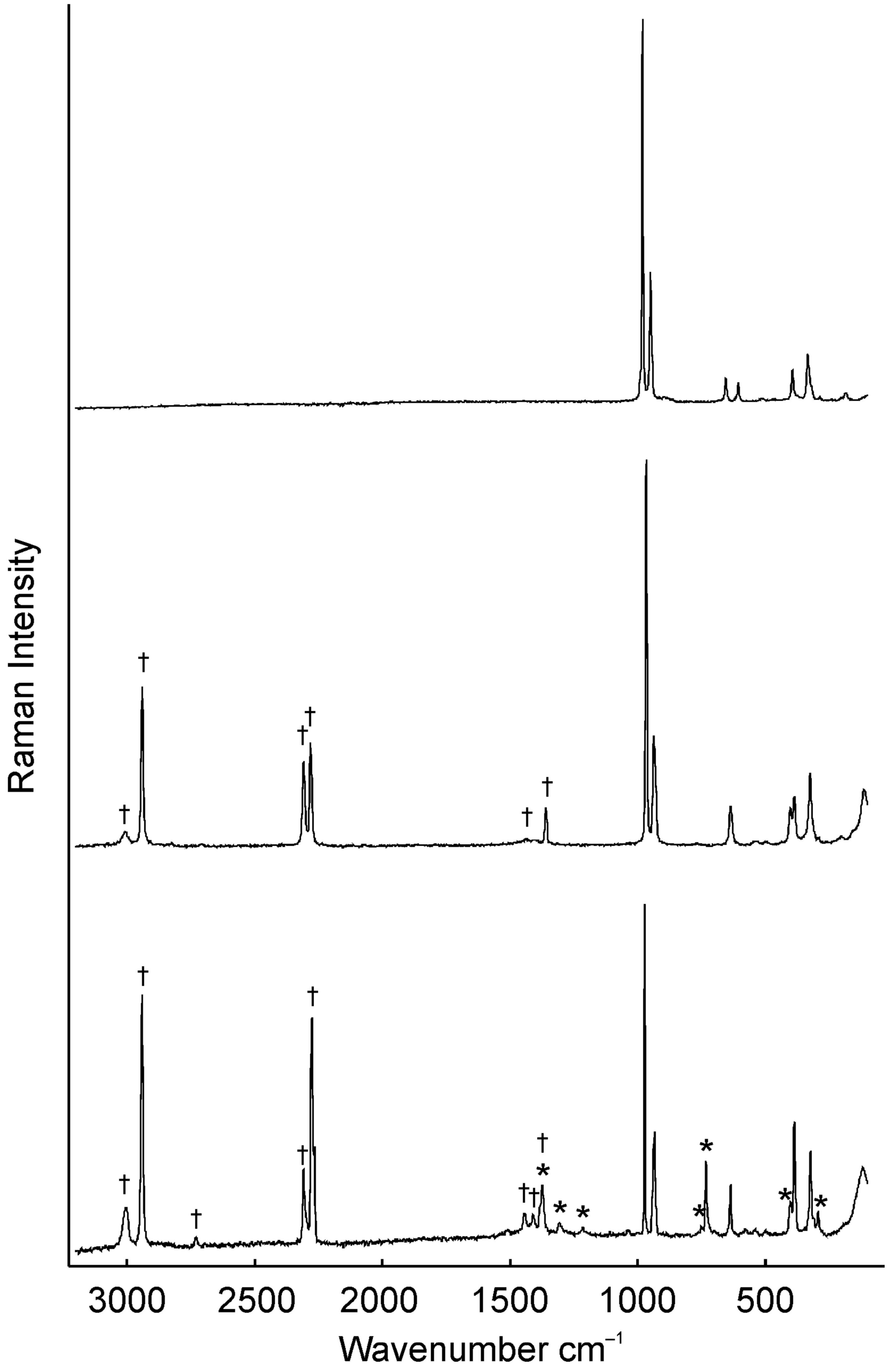

Figure 1 Raman spectra of Ag[ReO_2F_4] (upper trace), [$Ag(CH_3CN)_2$][ReO_2F_4] (middle trace), and [$Ag(CH_3CN)_4$][ReO_2F_4] (lower trace). Asterisks (*) denote bands arising from the FEP sample tube. Daggers (†) denote bands arising from the CH_3CN ligand.

Table 1 Raman Frequencies (cm^{-1}) and Tentative Assignments of $[Ag(CH_3CN)_4][ReO_2F_4]$, $[Ag(CH_3CN)_2][ReO_2F_4]$, $Ag[ReO_2F_4]$, and CH_3CN.

$[Ag(CH_3CN)_4][ReO_2F_4]$[a]	$[Ag(CH_3CN)_2][ReO_2F_4]$	$Ag[ReO_2F_4]$	CH_3CN[b]	Tentative Assignment
3007(13)	3006(3)		3001(7)	ν_{as}(C−H)
2941(76)	2940(42)		2943(100)	ν_s(C−H)
			2888(2)	Combination bands
			2847(2)	
2730(5)			2732(3)	
2308(23)	2308(23)		2293(5)	
2276(70) 2266(30)	2281(28)		2253(60)	ν(C≡N)
			2204(1)	Combination band
1443(5)			1443(3)	
1410(4)			1416(2)	$\delta_{as}(CH_3)$
	1360(11)		1375(6)	$\delta_s(CH_3)$
1038(1)				
973(100)	967(100)	981(100)		$\nu_s(ReO_2)$
939(28)	938(29)	951(34)		$\nu_{as}(ReO_2)$
934(33)			919(18)	ν(C−C)
636(16)	637(11)	655(6)		ν_s(ReF_2c,c + ReF_2c,t)
		607(5)		ν_{as}(ReF_2c,c)
402(10)	403(10)		380(10)	δ(C−C≡N)
387(35)[b]	387(14)	394(8)		$\delta_{sciss}(ReO_2)$
324(26)	326(19)	334(12)		sym comb of *cis/trans* ReF_2 scissor
	115(15)	185(2)		antisym comb of *cis/trans* ReF_2 scissor

[a] Signals from the FEP sample tube were observed at FEP: 1373(15), 1307(2), 1216(1), 733(23), 387(35), 294(6) cm^{-1}. [b] From reference 17.

The Raman spectrum of $[Ag(CH_3CN)_4][ReO_2F_4]$ contains signals associated with coordinated acetonitrile, as well as the $ReO_2F_4^-$ anion. The most intense band at 973 cm^{-1} and the band at 939 cm^{-1} can be assigned to the $\nu_s(ReO_2)$ and the $\nu_{as}(ReO_2)$ modes, respectively. These bands appear at the same frequency as those found in the previously reported Cs^+ and $N(CH_3)_4^+$ salts.[6] The $\nu_s(CH_3)$ mode has remained essentially un-shifted at 2941 cm^{-1} relative to that of neat liquid CH_3CN (2943 cm^{-1}).[17] The two C≡N stretching bands are significantly shifted to higher frequencies of 2276 and 2266 cm^{-1} compared to 2253 cm^{-1} found in neat liquid CH_3CN, reflecting the coordination of CH_3CN to the silver cation. The increase in the C≡N stretching frequency of acetonitrile upon complexation with metal cations is a well-documented phenomenon.[16,17] The observation of two C≡N stretching bands for the $[Ag(CH_3CN)_4]^+$ cation can be explained by the Raman active symmetric and asymmetric C≡N stretching modes that transform as the irreducible representations A_1 and T_2 in the T_d point group, respectively.

After removal of volatiles at room temperature under dynamic vacuum, the $\nu_s(ReO_2)$ band is shifted to a slightly lower frequency (967 cm^{-1}), and the signals associated with acetonitrile decreased in relative intensities. The C≡N stretching band has been shifted to an even higher frequency (2281 cm^{-1}) compared to that of $[Ag(CH_3CN)_4][ReO_2F_4]$ (2276 cm^{-1}), exhibiting a larger complexation shift than the tetrakisacetonitrile complex. These observations are in agreement with the change of the coordination geometry from tetrahedral to linear about the Ag^+ cation in $[Ag(CH_3CN)_2][ReO_2F_4]$, which is a commonly observed coordination mode of Ag^+. The low frequency of the $\nu_s(ReO_2)$ mode suggests that there is no significant interaction between the anion and the cation, as the frequency of this band shifts to higher wavenumbers as the cation becomes more Lewis acidic (987 cm^{-1} for K^+, 1011 cm^{-1} for Na^+).[6] The Raman spectrum of $Ag[ReO_2F_4]$ only contains peaks associated with the $ReO_2F_4^-$ moiety. The most intense band at 981 cm^{-1} was assigned to the $\nu_s(ReO_2)$ mode, which is at a higher frequency relative to the salts which contain CH_3CN coordinated to Ag^+, suggesting cation-anion interactions. This is corroborated by the significant increase in frequency of the $\nu_{as}(ReO_2)$ mode from 938 cm^{-1} ($[Ag(CH_3CN)_2][ReO_2F_4]$), to 951

cm^{-1} in $Ag[ReO_2F_4]$. The Raman spectrum most closely resembles that of the previously reported potassium salt.[6]

The Raman spectrum of $[N(CH_3)_4][IOF_4]$ is depicted in Figure 2, and vibrational frequencies and tentative assignments are listed in Table 2. The spectrum contains signals associated with the $N(CH_3)_4^+$ cation and the IOF_4^- anion. The bands associated with the $N(CH_3)_4^+$ moiety were assigned based on previous assignments of other tetramethylammonium salts.[18] The bands associated with the IOF_4^- anion were assigned based on the assignments for the previously reported $Cs[IOF_4]$ salt.[12] The most intense band in the Raman spectrum at 901 cm^{-1} can be assigned to the $\nu(I–O)$ mode, and is in good agreement with that of the $Cs[IOF_4]$ salt (889 cm^{-1}). The $\nu_s(IF_4)$ in-phase mode was assigned to the band at 526 cm^{-1} and is also in good agreement with the $Cs[IOF_4]$ salt (528 cm^{-1}).

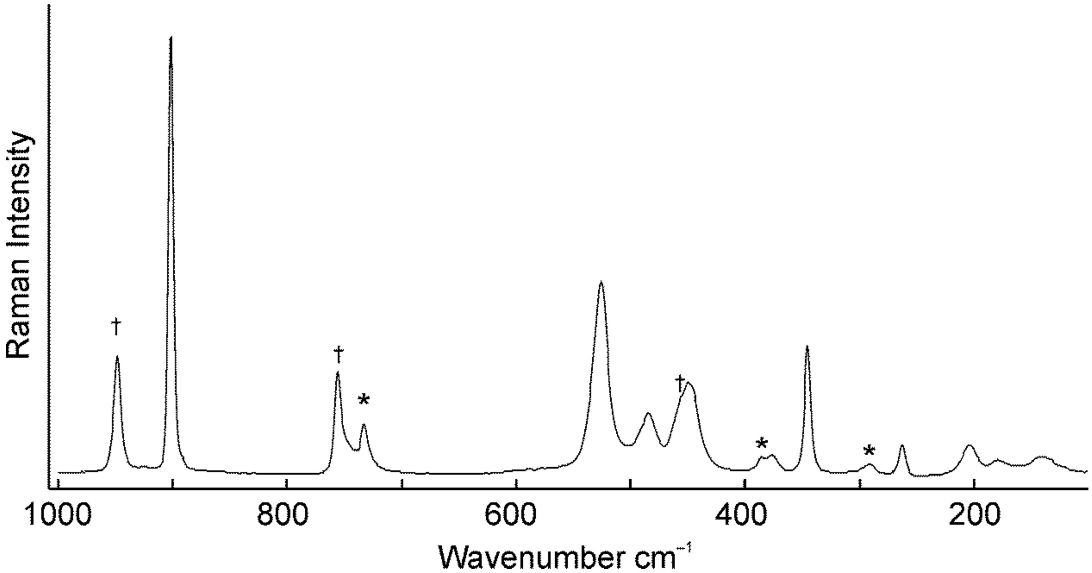

Figure 2 Raman spectrum of $[N(CH_3)_4][IOF_4]$. Asterisks (*) denote bands arising from the FEP sample tube. Daggers (†) denote bands arising from the $N(CH_3)_4^+$ cation.

Table 2 Raman Frequencies (cm^{-1}) and Tentative Assignments of $[N(CH_3)_4][IOF_4]$.

$[N(CH_3)_4][IOF_4]$	$Cs[IOF_4]^b$	Assignment
3039(25)		C–H stretch
2980(11)		
2960(23)		
2920(9)		
2882(5)		
2811(6)		
1531(1)		CH_3 deformation
1497(2)		
1470(33)		
1464(24)		
1412(7)		
1286(4)		C–N stretching modes
1175(6)		
1070(2)		
948(28)		$N(CH_3)_4^+$
901(100)	889(90)	•(I–O)
756(24)		$\bullet_s(NC_4)$
526(45)	528(100)	$\bullet_s(IF_4)$ in phase
484(15)	475(64)	$\bullet_s(IF_4)$ out of phase
449(22)		
376(5)		$\delta_s(NC_4)$
345(28)	360(25)	$\delta(OIF_4)$
263(7)	270sh	$\delta_s(IF_4)$ umbrella
204(8)	220sh	$\delta_s(IF_4)$ in plane
180(3)		
143(4)		$\delta_{as}(IF_4)$ in plane

[a] Signals from the FEP sample tube were observed at: 1380(3), 1214(1), 733(13), 526(overlap), 385(5), 291(3) cm^{-1}. [b] Reference 12.

The Raman frequencies and intensities for the known $IO_2F_4^-$ anion agree very well with what has previously been reported by Gillespie and Krasznai,[19] Christe *et al.*,[14] and Boatz *et al.*[15] The Raman spectrum contains signals associated with both the *cis*- and *trans*-$IO_2F_4^-$ anion.

2.2. X-ray Crystallography

Plate-shaped, multiply twinned crystals of $[Ag(CH_3CN)_4][ReO_2F_4]\cdot 2CH_3CN$ grew from CH_3CN at low temperature. Attempts to grow single crystals were unsuccessful. Selected crystallographic parameters and selected metric parameters for $[Ag(CH_3CN)_4][ReO_2F_4]\cdot 2CH_3CN$ are listed in Tables 3 and 4, respectively. The structure consists of well separated $ReO_2F_4^-$ anions, which adopt the *cis* conformation, and a silver cation coordinated by four acetonitrile ligands, forming a tetrahedral geometry around silver with two acetonitrile molecules per formula unit co-crystallizing in this salt (see Figure 3). The *cis*-$ReO_2F_4^-$ anion adopts a distorted octahedral geometry, in which the axial fluorines are pushed towards the equatorial fluorines. The ReF_{2ax} moiety lies in a mirror plane, and therefore the equatorial Re−O bonds as well as the $Re-F_{eq}$ bonds are crystallographically equivalent. The bond lengths agree well with those of the previously reported Li^+ salt. The Li^+ cation has six Li---F (2.04(3) to 2.108(7) Å) contacts in an octahedral geometry.[6] The Re−O bonds (1.679(9) Å) are significantly shorter than the $Re-F_{eq}$, trans to the Re−O bonds, (1.949(7) Å) and the $Re-F_{ax}$ bonds (1.918(10), 1.854(10) Å). These values agree with the $Li[ReO_2F_4]$ salt ($Re-F_{eq}$ = 1.867(8) Å and $Re-F_{ax}$ = 2.002(7) Å), except for the distortion of one of $Re-F_{ax}$ bonds.[6] The *cis*-dioxo arrangement is favoured in Re(VII) oxide fluoride species and has been thoroughly studied by vibrational and ^{19}F NMR spectroscopies.[6,20] For the $[Ag(CH_3CN)_4][ReO_2F_4]\cdot 2CH_3CN$ salt, no significant cation-anion contacts are observed, since acetonitrile ligands separate the cations from the anions. The limited number of crystal structures, which contain four CH_3CN ligands tetrahedrally coordinated to Ag^+ cations, contain counter-anions which are weakly coordinating such as BF_4^- or ClO_4^-.[21,22]

Table 3 Crystal Data Collection Parameters and Results for $[Ag(CH_3CN)_4][ReO_2F_4]\cdot 2CH_3CN$.

Compound	$[Ag(CH_3CN)_4][ReO_2F_4]\cdot 2CH_3CN$
Empirical Formula	$H_{18}C_{12}N_6O_2F_4AgRe$
Formula weight, g mol^{-1}	648.39
Temperature, K	153
Wavelength, Å	0.71073
Crystal System	Orthorhombic
Space Group	$Pmn2_1$
Unit Cell Dimensions	a = 13.408(4) Å
	b = 8.853(4) Å
	c = 8.872(7) Å
Volume	1053.1(10)
Z	2
Density (calculated), g cm^{-3}	2.045
Crystal Size, mm^3	0.09 × 0.23 × 0.41
Theta Range for data collection	27.3 to 2.3
Independent Reflections	1299
Parameters refined	137
Goodness-of-fit on F^2	1.24
Refine Diff $\Delta\rho_{max}$ e $Å^{-3}$	1.42
Refine Diff $\Delta\rho_{min}$ e $Å^{-3}$	−2.45
$R_1, I > 2\sigma(I)^a$	0.030
wR_2 $(F^2)^a$	0.081

$^{a}R_1 = \bullet||F_o| - |F_c||/\bullet|F_o|$; $wR_2 = [\bullet w(F_o^2 - Fc^2)^2/\bullet w(F_o^4)]^{1/2}$.

Table 4 Selected metric parameters for $[Ag(CH_3CN)_4][ReO_2F_4]\cdot 2CH_3CN$

Bond Lengths (Å)			
Re(1)−O(1)	1.679(9)	N(1)−C(1)	1.117(19)
Re(1)−F(1)	1.854(10)	C(1)−C(2)	1.52(2)
Re(1)−F(2)	1.949(7)	N(2)−C(3)	1.17(2)
Re(1)−F(3)	1.918(10)	C(3)−C(4)	1.39(3)
Ag(1)−N(1)	2.290(14)	N(3)−C(5)	1.118(14)
Ag(1)−N(2)	2.204(18)	C(5)−C(6)	1.441(15)
Ag(1)−N(3)	2.289(10)	N(4)−C(7)	1.143(17)
		C(7)−C(8)	1.438(18)
Bond Angles (°)			
O(1)−Re(1)−O(1)^{i}	101.4(7)	N(1)−Ag(1)−N(2)	104.5(6)
O(1)−Re(1)−F(1)	96.4(4)	N(1)−Ag(1)−N(3)	108.4(3)
O(1)−Re(1)−F(2)^{i}	168.6(4)	N(1)−Ag(1)−N(3)^{i}	108.4(3)
O(1)−Re(1)−F(3)	92.1(4)		

Symmetry code: (i) –x+1, y, z

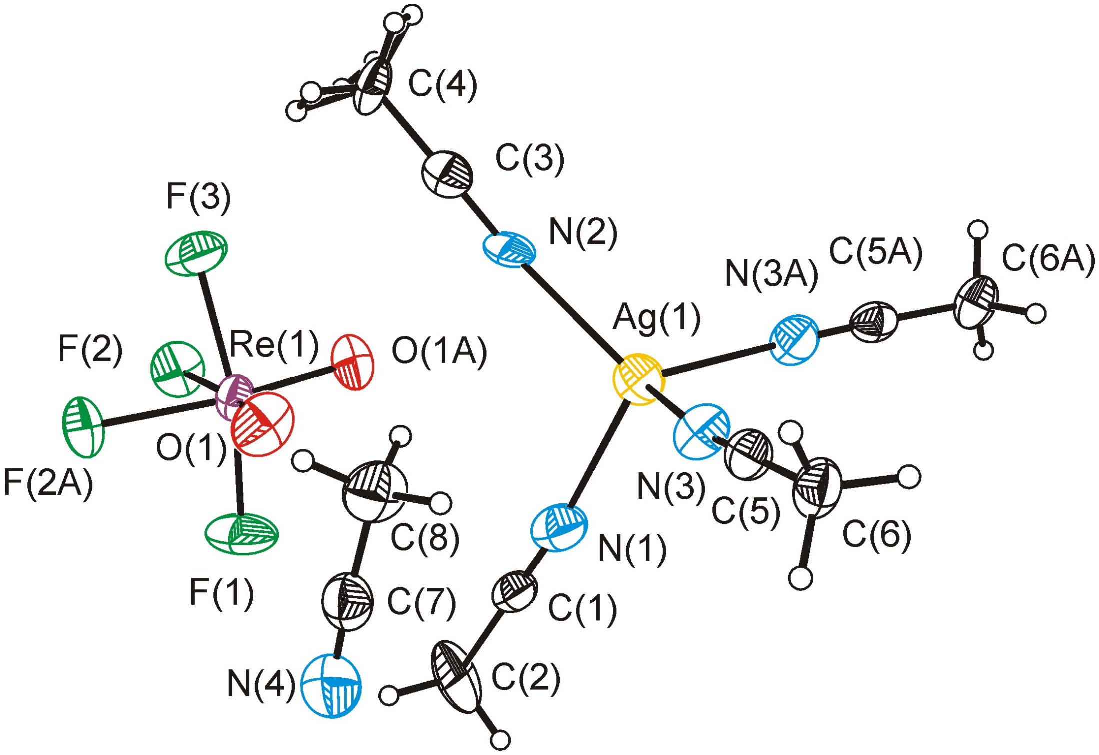

Figure 3 Thermal ellipsoid plot of $[Ag(CH_3CN)_4][ReO_2F_4]\cdot 2CH_3CN$. Thermal ellipsoids are set to 50% probability.

3. Conclusions

The reaction of main-group and transition-metal oxoanions with SF_4 conveniently formed Re^{VII}, I^{V}, and I^{VII} oxide fluoride anions. These reactions occur in acetonitrile or anhydrous HF and give quantitative yields in a single step. The byproducts and solvents are easily removed under dynamic vacuum at low temperatures, or in the case of the $[Ag(CH_3CN)_x]^+$ cation, upon mild heating. The $Ag[ReO_2F_4]$ salt was characterized by Raman spectroscopy. Although the $Ag[ReO_2F_4]$ salt had been previously prepared, it had only been characterized by elemental analysis. The new $[Ag(CH_3CN)_4][ReO_2F_4]\cdot 2CH_3CN$ salt was characterized by low-temperature Raman and X-ray crystallography. The new $[N(CH_3)_4][IOF_4]$ salt was synthesized and characterized by Raman spectroscopy, while $K[IO_2F_4]$ is now accessible in a one-step reaction.

4. Experimental

4.1 Materials and Apparatus

All volatile materials were handled on a Pyrex vacuum line equipped with glass/Teflon J. Young valves. Nonvolatile materials were handled in the dry nitrogen atmosphere of a dry box (Omni Lab, Vacuum Atmospheres).

Acetonitrile solvent (Baker, HPLC Grade) was purified according to the standard literature method.[23]

4.2 Preparation of $[Ag(CH_3CN)_x][ReO_2F_4]$ and $[Ag(CH_3CN)_x][ReO_2F_4]$, ($x = 0, 2, 4$)

Inside the dry box, 0.131 g (0.366 mmol) of $Ag[ReO_4]$ was loaded into a ¼-in. o.d. FEP tube equipped with a Kel-F valve. Excess acetonitrile (0.207 g, 5.04 mmol) was vacuum distilled onto the solid $Ag[ReO_4]$. The reactor was agitated at room temperature to dissolve the solid. Excess SF_4 (0.229 g, 2.12 mmol) was vacuum distilled onto the frozen mixture at –196 °C. After warming to and agitation at room temperature, a pale yellow slurry was obtained. Volatiles were removed under dynamic vacuum at –40 °C for 3.5 h, yielding 0.222 g of solid material, corresponding to a Ag^+ : CH_3CN ratio of 1: 5.0. Removal of volatiles for 1.5 h at –35 °C, gave 0.214 g of solid, (Ag^+ : CH_3CN ratio of 1: 4.5). A low-temperature the Raman spectrum of this sample did not show any signals associated with uncoordinated CH_3CN. Pumping on the sample at room temperature yielded 0.177 g of a pale yellow solid (Ag^+ : CH_3CN ratio of 1: 2.0), identified by Raman spectroscopy as $[Ag(CH_3CN)_2][ReO_2F_4]$. Removal of volatiles at 70 °C yielded 0.148 g of $Ag[ReO_2F_4]$. ^{19}F NMR (CH_3CN, unlocked, 282.4 MHz, δ [ppm]): –54.0 (t, F_{ct}), –63.7 (t, (F_{cc}), $^2J(^{19}F_{ct}\text{-}^{19}F_{cc}) = 87$ Hz.

4.3 Preparation of $[N(CH_3)_4][IOF_4]$

Inside the dry box, 0.072 g (0.29 mmol) of $[N(CH_3)_4][IO_3]$ was loaded into a ¼-in. o.d. FEP tube equipped with a Kel-F valve. Excess acetonitrile (0.563 g, 8.90 mmol) was vacuum distilled onto the solid $[N(CH_3)_4][IO_3]$. The reactor was agitated at room temperature, and only a small amount of solid dissolved. Excess SF_4 (0.466 g, 4.31 mmol) was distilled onto the frozen mixture at –196 °C. Warming to –40 °C caused the solid to bubble, and the solution to turn light yellow. Warming and agitation at room temperature caused the solution to turn a light orange. The volatiles were removed at –40 °C, yielding 0.088 g of colourless solid. ^{19}F NMR (CH_3CN, unlocked, 282.4 MHz, δ [ppm]): 10.6 (s).

4.4 Preparation of $K[IO_2F_4]$

Inside the dry box, 0.081 g (0.35 mmol) of KIO_4 was loaded into a ¼-in. o.d. FEP tube equipped with a Kel-F valve. Approximately 0.1 mL aHF was vacuum distilled on to the solid, which partially dissolved the solid. Excess SF_4 (0.227 g, 2.10 mmol) was vacuum distilled onto the frozen mixture at –196 °C. Warming the reaction mixture to ambient temperature caused the remaining solid to dissolve upon agitation, forming a clear colourless solution. The solvent was removed under dynamic vacuum at –78 °C, yielding 0.094 g (0.34 mmol) of colourless $K[IO_2F_4]$. ^{19}F NMR (HF, unlocked, 282.4 MHz, δ [ppm]): 64.4 (s, $4F_{trans}$), 86.9 (s, $2F_{cis}$), resonance for other 2 F environment for *cis*-isomer overlaps with F_{trans} resonance, approximate ratio of *trans*-$[IO_2F_4]^-$ to *cis*-$[IO_2F_4]^-$ from integration = 2.4 to 1. Raman (cm^{-1}): 1078(4); 875(2), (*cis* $\nu_{as}(IO_2)$); 856(19), (*cis* $\nu_{sym}(IO_2)$); 819(100), (*trans* $\nu_{sym}(IO_2)$); 797(2), (KIO_4); 609(13), (*cis* $\nu_{sym}(IF_{2eq})$); 577(41), (*trans* $\nu_{sym}(IF_4)_{in\ phase}$); 397(24), (*cis* $\delta_{sciss}(IO_2)$); 381(37), (*trans* $\delta(OIF_4O)$; 333(10), (*cis* $\nu_{torsion}(IO_2)$); 260(9), (*trans* $\nu_s(IF_4)_{in\ plane}$).

4.5. Vibrational Spectroscopy

The Raman spectra were recorded on a Bruker RFS 100 FT Raman spectrometer with a quartz beam splitter, a liquid-nitrogen-cooled Ge detector, and a low-temperature accessory. The backscattered (180°) radiation was sampled. The actual usable Stokes range was 50 to 3500 cm^{-1} with a spectral resolution of 2 cm^{-1}. The 1064-nm line of an Nd:YAG laser was used for excitation of the sample. The low-temperature (–100 °C) Raman spectra of $[Ag(CH_3CN)_4][ReO_2F_4]$ was recorded in a 4-mm FEP tube. The room temperature Raman spectra of $[Ag(CH_3CN)_x][ReO_2F_4]$ (x = 0, 2), $K[IO_2F_4]$, and $[N(CH_3)_4][IOF_4]$ were recorded on powdered samples in sealed melting point capillaries using a laser power of 150 mW (240 mW for $Ag[ReO_2F_4]$).

4.6. X-ray Crystallography

Slow cooling of a solution of $Ag[ReO_2F_4]$ in CH_3CN solvent from room temperature to –40 °C lead to the formation of large plate-like crystals. After removal of the removal of most of the volatiles at –40 °C, crystals were selected at low temperature under a stream of dry cold nitrogen as previously described.[24] The crystals were centered on a Bruker SMART APEX II diffractometer, controlled by the APEX2 Graphical User Interface software[25] using Mo Kα radiation ($\lambda = 0.71073$ Å) from a fine-focus tube. All crystals that were screened were multiply twinned. After finding the unit cell of the major component, three more components were indexed using the program CELL_NOW, after which reflections still remained that were not included.[26] After integration of these four components, TWINABS was used for scaling.[27] The structure was solved using the intrinsic method, and refined by the least-squares method on F^2 using SHELXL.[28]

Crystallographic data have been deposited with the Cambridge Crystallographic

Data Center, CCDC 1008793. Copies of the data can be obtained free of charge from CCDC via http://www.ccdc.cam.ac.uk.

Acknowledgements

We thank the Natural Sciences and Engineering Research Council of Canada and the University of Lethbridge for support of this work.

References

[1] W. Dmowski, Introduction of Fluorine Using Sulfur Tetrfluoride and Analogs, in: B. Baasner, H. Hagemann, J. C. Tatlow (Eds.), Organo-Fluorine Compounds, Methods of Organic Chemistry, Houben-Weyl, Vol. E10a, Thieme, Stuttgart, 2000, ch. 8, pp. 321-431.

[2] A. L. Oppegard, W. C. Smith, E. L. Muetterties, V. A. Engelhardt, J. Am. Chem. Soc. 82 (1960) 3835-3838.

[3] W. C. Smith, V. A. Engelhardt, J. Am. Chem. Soc. 82 (1960) 3838-3840.

[4] M. Gerken, H. P. A. Mercier, G. J. Schrobilgen, Syntheses and Structures of the Oxide Fluorides of the Main-Group and Transition Metal Elements, in: T. Nakajima, B. Zemva, A. Tressaud Eds.) Advanced Inorganic Fluorides, Elsevier, Lausanne, 2000, ch. 5, pp. 117-174.

[5] R. D. Peacock, J. Chem. Soc. (1955) 602-603.

[6] W. J. Casteel, D. A. Dixon, N. LeBlond, P. E. Lock, H. P. A. Mercier, G. J. Schrobilgen, Inorg. Chem. 38 (1999) 2340-2358.

[7] A. K. Brisdon, J. H. Holloway, E. G. Hope, J. Fluorine Chem. 89 (1998) 35-37.

[8] J. Supeł, R. Marx, K.Seppelt, Z. Anorg. Allg. Chem. 631 (2005) 2979-2986.

[9] H. Selig, U. El-Gad, J. Inorg. Nucl. Chem. 35 (1973) 3517-3522.

[10] J. B. Milne, D. M. Moffett, Inorg. Chem. 15 (1976) 2165-2169.

[11] K .O. Christe, R. D. Wilson, E. C. Curtis, W. Kuhlmann, W. Sawodny, Inorg. Chem. 17 (1978) 533-538.

[12] K. O. Christe, W. W. Wilson, R. D. Wilson, Inorg. Chem. 28 (1989) 904-908.

[13] R. R. Ryan, L. B. Asprey, Acta Crystallogr. B 28 (1972) 979-981.

[14] K. O. Christe, R. D. Wilson, C. J. Schack, Inorg. Chem. 20 (1981) 2104-2114.

[15] J. A. Boatz, K. O. Christe, D. A. Dixon, B. A. Fir, M. Gerken, R. Z. Gnann, H. P. A. Mercier, G. J. Schrobilgen, Inorg. Chem. 42 (2003) 5282-5292.

[16] J. Reedijk, A. P. Zuur, W. L. Groeneveld, Recl. Trav. Chim. Pays-Bas 86 (1967) 1127-1137.

[17] J. Nieboer, W. Hillary, X. Yu, H. P. A. Mercier, M. Gerken, Inorg. Chem. 48 (2009) 11251-11258.

[18] G. Kabisch, J. Raman Spectrosc. 9 (1980) 279-285.

[19] R. J. Gillespie, J. P. Krasznai, Inorg. Chem. 16 (1977) 1384-1392.

[20] W. Kuhlmann, W. Sawodny, J. Fluorine Chem. 9 (1977) 341-357.

[21] A. Aly, B.Walfort, H. Lang, Z. Kristallogr. - New Cryst. Struct. 219 (2004) 489-491.

[22] P. G. Jones, E. Bembenek, Z. Kristallogr. 208 (1993) 489-491.

[23] J. M. Winfield, J. Fluorine Chem. 25 (1984) 91-98.

[24] M. Gerken, D. A. Dixon and G. J. Schrobilgen, Inorg. Chem. 39 (2000) 4244-4255.

[25] APEX 2, Version 2014.3-0; Bruker AXS Inc.; Madison, WI, 2005-2014.

[26] G. M. Sheldrick, CELL_NOW, Version 2008/4, University of Göttingen, Germany, 2008.

[27] TWINABS, Version 2012/1; Bruker AXS Inc.; Madison, WI, 2012.

[28] G. M. Sheldrick, SHELXTL-2014, University of Göttingen, Germany, 2014.